

Fracton physics of spatially extended excitations. II. Polynomial ground state degeneracy of exactly solvable models

Meng-Yuan Li¹ and Peng Ye^{1, *}

¹*School of Physics and State Key Laboratory of Optoelectronic Materials and Technologies, Sun Yat-sen University, Guangzhou, 510275, China*

(Dated: Wednesday 14th April, 2021)

In our previous work [Phys. Rev. B 101,245134 (2020)], we constructed a series of higher-dimensional exactly solvable fracton ordered models with spatially extensive excitations whose mobility and deformability are restricted. In this paper, we proceed further to propose a combinatorial method to calculate their ground state degeneracy (GSD). By decomposing a state into a collection of subsystem ground state sectors, we find that a ground state can be reconstructed from a consistent collection of subsystem data. As a result, we find that GSD formulas (after taking logarithm) have very diverse polynomial-dependency on the sizes. Inspired from known results about the relation between GSD of X-cube models and the first Betti numbers with \mathbb{Z}_2 coefficients of leaves, we expect that the coefficients in the polynomials of these higher-dimensional models may reflect some mathematical properties in higher dimensions.

CONTENTS

I. Introduction	1
II. Preliminaries	2
A. Geometric Notations	2
B. Review of $[d_n, d_s, d_l, D]$ Models	3
C. Review of GSD Computation	5
III. GSD of $[d_n, d_s, d_l, D]$ Models	5
A. Representing Ground States with Low Dimensional Data	5
1. Decomposition of Lattices	6
2. Decomposition of Configurations and Operators	6
3. Decomposition of Ground State Sectors	7
B. General Procedures of the Calculation	8
C. Computation of the GSD of X-cube Model as a Coloring Problem	8
D. GSD of $[0, 1, 2, D]$ and $[D - 3, D - 2, D - 1, D]$ Models	11
1. Isotropic Lattice	11
2. Anisotropic Lattice	11
E. Remarks about GSD	12
IV. Conclusion	12
Acknowledgements	12
References	13

I. INTRODUCTION

For many years, topological orders which support fractionalized excitations have been central to the discovery

of matters beyond the symmetry breaking paradigm[1, 2]. One of the most famous example of topological ordered systems is fractional quantum Hall effect (FQHE), which supports topological excitations carrying fractionalized charges. And due to the fractionalization, certain number of such topological excitations must be created or annihilated simultaneously. For example, in 2D toric code model, topological excitations are generated by string operators, so two excitations at the two endpoints of one string must be created or annihilated simultaneously[3]. The string picture captures the topological nature of excitations in a natural way. While recently, a new kind of orders was found, which presents properties beyond the scope of conventional topological orders, that is the fracton order[4, 5]. Even at the absence of disorders, topological excitations in fracton order systems can be spatially restricted in certain points or subspaces of the whole system. As besides the theoretical novelty of subdimensional excitations, it is believed that fracton order systems may be utilized as stable topological quantum memory. Since has been proposed, fracton orders have attracted general interests from various fields, such as quantum information, quantum dynamics and high energy physics[4–75].

For now, most works about fracton orders are focusing on point-like excitations with restricted mobility. While in 3D and higher dimensional pure topological orders, spatially extended excitations, such as strings and membranes, have also attracted a lot of attentions[76–100]. In our previous work [71], we proposed a series of exactly solvable lattice models (dubbed as $[d_n, d_s, d_l, D]$ models. Here d_n, d_s, d_l and D are 4 number of dimensions. See Sec. II B for more details), and discussed about the excitations in these models. To our surprise, these models contain not only point-like subdimensional excitations, but also spatially extended excitations (such as strings, membranes and etc.) with restricted mobility and deformability. Except for these excitations with usual shapes, we also found spatially extended excita-

* yepeng5@mail.sysu.edu.cn

tions with stable non-manifold-like shapes in some of such models, which are named as complex excitations for their unconventional topology. Besides, excitations with stable disconnected shapes are also discussed. Here “stable” means that for such excitations, due to the deformability restriction, their topology cannot be changed under any local unitary transformations. In conclusion, we classify the topological excitations in gapped fracton orders into 4 sectors, which are respectively trivial, simple, disconnected and complex excitations.

As ground state wave functions contains essential information of topological orders, ground state degeneracy (GSD) is also an important character of orders. Furthermore, in fracton orders, it has been found that GSD of certain models are no longer uniquely determined by the topology of the base manifold, but also depend on various topological and geometric properties, such as foliation[6, 7, 10–12, 25, 26, 56, 57, 101]. In this paper, we try to give a further discussion about the ground state degeneracy (GSD) of $[d_n, d_s, d_l, D]$ models. As another significant character that distinguishes fracton orders from conventional topological orders, we believe that the knowledge of GSD is necessary for us to obtain a more complete picture of fracton orders.

We propose a method to calculate the GSD of a subset of $[d_n, d_s, d_l, D]$ models, and our results show that the GSD of a subset of $[d_n, d_s, d_l, D]$ models (such as $[0, 1, 2, D]$ -models) becomes polynomial of the linear sizes of the system, as summarized in Table. I. As we shall demonstrate in Sec. III, the polynomial $\log_2 GSD$ of $[0, 1, 2, D]$ models may results from the multi-level foliation structures of the models ($D \geq 4$). Here multi-level foliation means that a ground state of a $[0, 1, 2, D]$ model restricted in a $(D - 1)$ -dimensional subspace is a $[0, 1, 2, D - 1]$ ground state, which also have a foliation structure. An exact definition of restriction of ground states is given in Sec. III A. In a series of works about foliated fracton orders, the coefficients of linear terms of $\log_2 GSD$ of X-cube models are identified as the first Betti numbers with \mathbb{Z}_2 coefficients of leaves[25]. Inspired from this result, we believe the coefficients of the terms in the polynomial $\log_2 GSD$ of a $[d_n, d_s, d_l, D]$ model may reflect certain mathematical properties of the system.

To compute the GSD of $[d_n, d_s, d_l, D]$ models, we propose a decomposition of base manifolds for $[d_n, d_s, d_l, D]$ models, which can be intuitively recognized as a class of foliation structures of different dimensions. Based on that, we construct the decomposition of spin configurations, stabilizers and ground states in $[d_n, d_s, d_l, D]$ models. And by proving that there is a one-to-one correspondence between a ground state sector in the fracton ordered model and a consistent collection of ground state sectors, we obtain the GSD with a combinatorial algorithm.

This paper is organized as follows. In Sec. II, we introduce the geometric concepts necessary to our proof and computation. After that, for interested readers, a brief review of X-cube and more general $[d_n, d_s, d_l, D]$

models is given in Sec. II B. In Sec. III, we demonstrate the concept of decomposition of spin configurations and states, and prove that for $[d_n, d_s, d_l, D]$ models satisfying certain conditions, their GSD can be obtained by counting consistent collections of subsystem ground state sectors. Then, we concretely calculate the GSD of several $[d_n, d_s, d_l, D]$ models, and briefly discuss a potential meaning of the results in mathematics. In Sec. IV, we give a brief summary of our computation of GSD and its potential implications, and tentatively discuss about some relevant questions yet to be solved.

II. PRELIMINARIES

A. Geometric Notations

To refer to high dimensional objects, here we find it is necessary to introduce a series of geometric notations. Besides, we also give a brief introduction of some basic concepts about foliation theory, to make the definition of $[d_n, d_s, d_l, D]$ models clear.

We begin with an introduction of a coordinate system. In this paper, as we mainly focus on cubic lattice, we can refer to a d -cube denoted as γ_d via the coordinate of its geometric center. Here a d -cube is a d -dimensional analog of a cube¹. Furthermore, by setting the lattice constant to be 1, the coordinate of a d -cube in a D -dimensional cubic lattice always contains $(D - d)$ integers and d half-integers. For example, in a 3-dimensional cubic lattice, we have $(0, 0, 0)$ refers to a 0-cube, $(\frac{1}{2}, 0, 0)$ refers to a 1-cube, $(\frac{1}{2}, \frac{1}{2}, 0)$ refers to a 2-cube, and $(\frac{1}{2}, \frac{1}{2}, \frac{1}{2})$ refers to a 3-cube.

Next, we explain the meaning of “nearest to”. In a D -dimensional cubic lattice, for $\gamma_{d_i} = (x_1, x_2, \dots, x_D)$ and $\gamma_{d_j} = (y_1, y_2, \dots, y_D)$, we say they are nearest to each other if and only if:

$$\begin{aligned} L_1(\gamma_{d_i}, \gamma_{d_j}) &\equiv |x_1 - y_1| + |x_2 - y_2| + \dots + |x_D - y_D| \\ &= \frac{|d_i - d_j|}{2}, \quad i \neq j, \\ L_1(\gamma_{d_i}, \gamma_{d_j}) &\equiv |x_1 - y_1| + |x_2 - y_2| + \dots + |x_D - y_D| \\ &= 1, \quad i = j. \end{aligned}$$

It is easy to check that this definition is consistent with the conventional definition. Moreover, given $d_i < d_j$, γ_{d_i} being inside γ_{d_j} is equivalent to that γ_{d_i} being nearest to γ_{d_j} . A more detailed introduction of this notation is given in Sec. II of Ref. [71].

Furthermore, in order to give an intuitive picture of the definition of $[d_n, d_s, d_l, D]$ models, here we give a heuristic introduction of foliation. For a more detailed discussion, see Ref. [102].

¹ For example, 0-cubes are vertices, 1-cubes are links, and 2-cubes are plaquettes.

TABLE I. $\log_2 GSD$ of different $[d_n, d_s, d_l, D]$ models of both isotropic and anisotropic lattices with periodic boundary conditions. The models above the horizontal line are isotropic, where L is the linear size of the lattices. The models below the horizontal line are anisotropic, where L_n is the linear size along the \hat{x}_n direction of the lattices. It is known that in X-cube model, the coefficients of the linear terms are the first Betti numbers of leaves. Therefore, these coefficients reflect the topological properties of leaves. While as we can see, in $[0, 1, 2, D]$ models with $D \geq 4$, except for the linear term, we also obtain terms of higher degrees. Moreover, in anisotropic models, there are also crossing terms between sizes along different directions. Such terms of higher degrees require further analysis to understand how they are related to the topological and geometric properties of the models.

Model	$\log_2 GSD$
X-cube	$6L - 3$
$[0, 1, 2, 4]$	$12L^2 - 12L + 4$
$[1, 2, 3, 4]$	$12L - 6$
$[0, 1, 2, D]$	$\sum_{n=0}^{D-2} D \times \binom{D-1}{n} (-1)^{D+n} L^n$
$[D-3, D-2, D-1, D]$	$\binom{D}{D-2} \times (2L - 1)$
X-cube	$2L_1 + 2L_2 + 2L_3 - 3$
$[0, 1, 2, 4]$	$2L_1L_2 + 2L_1L_3 + 2L_1L_4 + 2L_2L_3 + 2L_2L_4 + 2L_3L_4 - 3L_1 - 3L_2 - 3L_3 - 3L_4 + 4$
$[1, 2, 3, 4]$	$3L_1 + 3L_2 + 3L_3 + 3L_4 - 6$
$[0, 1, 2, 5]$	$2L_1L_2L_3 + 2L_1L_2L_4 + 2L_1L_2L_5 + 2L_2L_3L_4 + 2L_2L_3L_5 + 2L_3L_4L_5 + 2L_3L_4L_5 - 3L_1L_2 - 3L_1L_3 - 3L_1L_4 - 3L_1L_5 - 3L_2L_3 - 3L_2L_4 - 3L_2L_5 - 3L_3L_4 - 3L_3L_5 - 3L_4L_5 + 4L_1 + 4L_2 + 4L_3 + 4L_4 + 4L_5 - 5$
$[2, 3, 4, 5]$	$4L_1 + 4L_2 + 4L_3 + 4L_4 + 4L_5 - 10$

In general, foliation is partition of a manifold into a set of submanifolds, where the submanifolds are dubbed as leaves. For a regular foliation, where all leaves are of the same dimension, the dimension of leaves is defined as the dimension of the foliation. In this paper, as we only consider lattices defined on toric manifolds and regular foliations, we will treat leaves simply as sublattices. A pictorial demonstration of foliation is given in Fig. 2.

For foliated fracton orders, two systems belong to the same phase if they can be transformed to each other under addition or removal of subdimensional topologically ordered phases. Therefore, their physical properties, like ground state degeneracy, have direct relationship with their foliation structures. A large amount of Type-I fracton orders have been proved to be foliated fracton orders, like X-cube model and checkerboard model[10, 11, 58].

Last but not least, inspired by the idea of higher-order topological insulator[103], here we give a rough definition of higher-order boundary in cubic and hypercubic lattices, in order to refer to the higher-dimensional analogs of hinges of a cuboid.

Firstly, we consider the d -dimensional analogs of cuboid, denoted as S^d . For example, an S^1 is a straight string, an S^2 is a flat membrane, and an S^3 is a cuboid. See Ref. [71] for more details of S^n notations.

Then, for such an S^d , we can define its d_i -dimensional boundary as follows (here $d_i < d$ is assumed):

- The d_i -dimensional boundary of an S^d is composed of γ_{d_i} 's.
- A γ_{d_i} belongs to the d_i -dimensional boundary of the S^d if and only if it is nearest to exactly one γ_d in the S^d .

We can check that such a definition is consistent with our intuition. For example, the 0-dimensional boundary

of a plaquette is composed of the 4 vertices of the plaquette, and the the 1-dimensional boundary of a common cube is composed of the 12 hinges of the cube. While for a cuboid extended along one spatial direction, we can see that its 1-dimensional boundary is composed of only 4 hinges.

B. Review of $[d_n, d_s, d_l, D]$ Models

As we shall exemplify our GSD computing algorithm with the $[d_n, d_s, d_l, D]$ models proposed in [71], we believe it would be beneficial to give a review of the definition of the models at first.

$[d_n, d_s, d_l, D]$ models are defined on D -dimensional cubic lattice with $1/2$ -spins as basic degrees of freedom. A spin sit on the center of a γ_{d_s} . The Hamiltonian is defined as below:

$$H_{[d_n, d_s, d_l, D]} = -J \sum_{\{\gamma_D\}} A_{\gamma_D} - K \sum_{\{\gamma_{d_n}\}} \sum_l B_{\gamma_{d_n}}^l, \quad (1)$$

where $J, K > 0$ are coupling constants, a $B_{\gamma_{d_n}}^l$ term is the product of all z -components of spins which are both a) nearest to the γ_{d_n} and b) inside the d_l -dimensional leaf space (i.e. sublattice) l . While an A_{γ_D} term is the product of all x -components of spins which are nearest to the γ_D . In other words, in order to determine a $B_{\gamma_{d_n}}^l$ term for a given γ_{d_n} , firstly, we need to choose a d_l -dimensional sublattice l where γ_{d_n} is embedded, then find all d_s -cubes which are not only nearest to the γ_{d_n} but also totally embedded in l . Then the $B_{\gamma_{d_n}}^l$ is just the product of the z -components of all the spins on such d_s -cubes. Since for a $B_{\gamma_{d_n}}^l$ term, its location is determined by the subscript γ_{d_n} , we only need to label the leaf l by its

direction. For example, in X-cube model, where $d_l = 2$, we use $\langle \hat{x}_1 \hat{x}_2 \rangle$, $\langle \hat{x}_1 \hat{x}_3 \rangle$ and $\langle \hat{x}_2 \hat{x}_3 \rangle$ as the superscripts of B terms. See Eq. 2 for an instance.

According to the definition of the Hamiltonian, we can see that the numbers in the label of a $[d_n, d_s, d_l, D]$ model are just dimensions indices. In Ref. [71], it has been proved that a $[d_n, d_s, d_l, D]$ model is exactly solvable when d_n, d_s, d_l and D satisfy $\binom{d_l - d_n}{d_s - d_n} \bmod 2 = 0$ together with $d_n < d_s < d_l < D$.

And there are two specially interesting branches of such exactly solvable models, $[0, 1, 2, D]$ and $[D - 3, D - 2, D - 1, D]$. In this paper, we will mainly focus on these two branches of models.

In $[D - 3, D - 2, D - 1, D]$ models with $D \geq 4$, our previous work[71] find that there are extended excitations with fracton physics. That is to say, both mobility and deformability of spatially extended excitations (e.g. loop excitations and membrane excitations) in these models can be restricted. What's more, some topological excitations can even have non-manifold shapes. Such excitations with non-manifold-like shapes are dubbed as complex excitations. For complex excitations, as long as the connectivity of their shapes are preserved, they cannot be deformed to be manifold-like objects by any local unitary operators. Similarly, we can also define (intrinsically) disconnected excitations, whose shapes cannot be deformed to be connected by any local unitary operators. In conclusion, topological excitations in $[d_n, d_s, d_l, D]$ models can be classified into 4 sectors, which are respectively trivial excitations, simple excitations, disconnected excitations and complex excitations. The latter 2 sectors only exist in fracton orders.

For examples, we can consider the following models:

- *X-cube* $[0, 1, 2, 3]$ model In our notation, X-cube model is denoted as $[0, 1, 2, 3]$ (it means $d_n = 0$, $d_s = 1$, $d_l = 2$ and $D = 3$ in the general form of Hamiltonian Eq. 1). The Hamiltonian is composed of $B_{\gamma_0}^l$ and A_{γ_3} terms defined on vertices and cubes respectively. And since we have $d_l = 2$, such a $B_{\gamma_0}^l$ term equals to the product of 4 σ^z 's sitting on the 4 links which are (a) embedded in the plane l and (b) nearest to the vertex γ_0 . Similarly, an A_{γ_3} term is the product of 12 σ^x 's sitting on the 12 links that are nearest to the γ_3 . For example, for a common cubic lattice, we have

$$B_{(0,0,0)}^{\langle \hat{x}_1, \hat{x}_2 \rangle} = \sigma_{(0, \frac{1}{2}, 0)}^z \sigma_{(-\frac{1}{2}, 0, 0)}^z \sigma_{(\frac{1}{2}, 0, 0)}^z \sigma_{(0, -\frac{1}{2}, 0)}^z, \quad (2)$$

and

$$\begin{aligned} A_{(\frac{1}{2}, \frac{1}{2}, \frac{1}{2})} &= \sigma_{(0,0,\frac{1}{2})}^x \sigma_{(0,1,\frac{1}{2})}^x \sigma_{(1,0,\frac{1}{2})}^x \sigma_{(1,1,\frac{1}{2})}^x \\ &\quad \sigma_{(0,\frac{1}{2},0)}^x \sigma_{(0,\frac{1}{2},1)}^x \sigma_{(1,\frac{1}{2},0)}^x \sigma_{(1,\frac{1}{2},1)}^x \\ &\quad \sigma_{(\frac{1}{2},0,0)}^x \sigma_{(\frac{1}{2},0,1)}^x \sigma_{(\frac{1}{2},1,0)}^x \sigma_{(\frac{1}{2},1,1)}^x, \end{aligned} \quad (3)$$

where subscript coordinates like $(0, 0, 0)$ and $(1, 0, \frac{1}{2})$ respectively refer to a γ_0 and a γ_1 , as they

are exactly the geometric centers of these two objects. In X-cube model, we have fractons and lineons as fundamental excitations. These excitations respectively correspond to the eigenvalue flips of $B_{\gamma_0}^l$ and A_{γ_3} terms.

- $[0, 1, 2, 4]$ model The Hamiltonian of $[0, 1, 2, 4]$ model is composed of $B_{\gamma_0}^l$ and A_{γ_4} terms. And since we have $d_l = 2$, such a $B_{\gamma_0}^l$ term equals to the product of 4 σ^z 's sitting on the 4 links which are (a) embedded in the plane l and (b) nearest to the vertex γ_0 . Similarly, an A_{γ_4} term is the product of 32 σ^x 's sitting on the 32 links that are nearest to the γ_4 . For a common hypercubic lattice, we have

$$B_{(0,0,0,0)}^{\langle \hat{x}_1, \hat{x}_2 \rangle} = \sigma_{(0, \frac{1}{2}, 0, 0)}^z \sigma_{(-\frac{1}{2}, 0, 0, 0)}^z \sigma_{(\frac{1}{2}, 0, 0, 0)}^z \sigma_{(0, -\frac{1}{2}, 0, 0)}^z, \quad (4)$$

and

$$\begin{aligned} A_{(\frac{1}{2}, \frac{1}{2}, \frac{1}{2}, \frac{1}{2})} &= \sigma_{(0,0,\frac{1}{2},0)}^x \sigma_{(0,1,\frac{1}{2},0)}^x \sigma_{(1,0,\frac{1}{2},0)}^x \sigma_{(1,1,\frac{1}{2},0)}^x \\ &\quad \sigma_{(0,\frac{1}{2},0,0)}^x \sigma_{(0,\frac{1}{2},1,0)}^x \sigma_{(1,\frac{1}{2},0,0)}^x \sigma_{(1,\frac{1}{2},1,0)}^x \\ &\quad \sigma_{(\frac{1}{2},0,0,0)}^x \sigma_{(\frac{1}{2},0,1,0)}^x \sigma_{(\frac{1}{2},1,0,0)}^x \sigma_{(\frac{1}{2},1,1,0)}^x \\ &\quad \sigma_{(0,0,\frac{1}{2},1)}^x \sigma_{(0,1,\frac{1}{2},1)}^x \sigma_{(1,0,\frac{1}{2},1)}^x \sigma_{(1,1,\frac{1}{2},1)}^x \\ &\quad \sigma_{(0,\frac{1}{2},0,1)}^x \sigma_{(0,\frac{1}{2},1,1)}^x \sigma_{(1,\frac{1}{2},0,1)}^x \sigma_{(1,\frac{1}{2},1,1)}^x \\ &\quad \sigma_{(\frac{1}{2},0,0,1)}^x \sigma_{(\frac{1}{2},0,1,1)}^x \sigma_{(\frac{1}{2},1,0,1)}^x \sigma_{(\frac{1}{2},1,1,1)}^x \\ &\quad \sigma_{(0,0,0,\frac{1}{2})}^x \sigma_{(0,0,1,\frac{1}{2})}^x \sigma_{(0,1,0,\frac{1}{2})}^x \sigma_{(0,1,1,\frac{1}{2})}^x \\ &\quad \sigma_{(1,0,0,\frac{1}{2})}^x \sigma_{(1,0,1,\frac{1}{2})}^x \sigma_{(1,1,0,\frac{1}{2})}^x \sigma_{(1,1,1,\frac{1}{2})}^x. \end{aligned} \quad (5)$$

In $[0, 1, 2, 4]$ model, we have fractons and lineons as fundamental excitations. These excitations respectively correspond to the eigenvalue flips of $B_{\gamma_0}^l$ and A_{γ_4} terms.

- $[1, 2, 3, 4]$ model The Hamiltonian of $[1, 2, 3, 4]$ model is composed of $B_{\gamma_1}^l$ and A_{γ_4} terms. And since we have $d_l = 3$, such a $B_{\gamma_1}^l$ term equals to the product of 4 σ^z 's sitting on the 4 plaquettes which are (a) embedded in the 3-dimensional space l and (b) nearest to the link γ_1 . Similarly, an A_{γ_4} term is the product of 24 σ^x 's sitting on the 24 plaquettes that are nearest to the γ_4 . For a common hypercubic lattice, we have

$$B_{(0,0,0,\frac{1}{2})}^{\langle \hat{x}_1, \hat{x}_2, \hat{x}_4 \rangle} = \sigma_{(\frac{1}{2}, 0, 0, \frac{1}{2})}^z \sigma_{(-\frac{1}{2}, 0, 0, \frac{1}{2})}^z \sigma_{(0, \frac{1}{2}, 0, \frac{1}{2})}^z \sigma_{(0, -\frac{1}{2}, 0, \frac{1}{2})}^z, \quad (6)$$

and

$$\begin{aligned} A_{(\frac{1}{2}, \frac{1}{2}, \frac{1}{2}, \frac{1}{2})} &= \sigma_{(0,0,\frac{1}{2},\frac{1}{2})}^x \sigma_{(0,1,\frac{1}{2},\frac{1}{2})}^x \sigma_{(1,0,\frac{1}{2},\frac{1}{2})}^x \sigma_{(1,1,\frac{1}{2},\frac{1}{2})}^x \\ &\quad \sigma_{(0,\frac{1}{2},0,\frac{1}{2})}^x \sigma_{(0,\frac{1}{2},1,\frac{1}{2})}^x \sigma_{(1,\frac{1}{2},0,\frac{1}{2})}^x \sigma_{(1,\frac{1}{2},1,\frac{1}{2})}^x \\ &\quad \sigma_{(0,\frac{1}{2},\frac{1}{2},0)}^x \sigma_{(0,\frac{1}{2},\frac{1}{2},1)}^x \sigma_{(1,\frac{1}{2},\frac{1}{2},0)}^x \sigma_{(1,\frac{1}{2},\frac{1}{2},1)}^x \\ &\quad \sigma_{(\frac{1}{2},0,0,\frac{1}{2})}^x \sigma_{(\frac{1}{2},0,1,\frac{1}{2})}^x \sigma_{(\frac{1}{2},1,0,\frac{1}{2})}^x \sigma_{(\frac{1}{2},1,1,\frac{1}{2})}^x \\ &\quad \sigma_{(\frac{1}{2},0,\frac{1}{2},0)}^x \sigma_{(\frac{1}{2},0,\frac{1}{2},1)}^x \sigma_{(\frac{1}{2},1,\frac{1}{2},0)}^x \sigma_{(\frac{1}{2},1,\frac{1}{2},1)}^x \\ &\quad \sigma_{(\frac{1}{2},\frac{1}{2},0,0)}^x \sigma_{(\frac{1}{2},\frac{1}{2},0,1)}^x \sigma_{(\frac{1}{2},\frac{1}{2},1,0)}^x \sigma_{(\frac{1}{2},\frac{1}{2},1,1)}^x. \end{aligned} \quad (7)$$

In [1, 2, 3, 4] model, we have fractons and (1, 2)-type excitations as fundamental excitations. These excitations respectively correspond to the eigenvalue flips of $B_{\gamma_1}^l$ and A_{γ_4} terms. Here (1, 2)-type means that the excitation is intrinsically 1-dimensional (i.e. it is a string), and its mobility and deformability are restricted in a 2-dimensional subspace. For more details of (m, n) -type excitations, see Ref. [71].

A pictorial demonstration of such an A_{γ_4} term is given in Fig. 1.

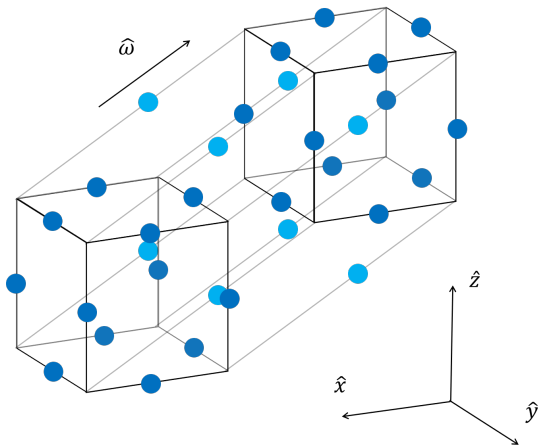


FIG. 1. Pictorial demonstration of an A_{γ_4} term in [0, 1, 2, 4] model on a 4-dimensional lattice. Spins are located on links, and they are represented by blue dots. While for clarity, spins along the fourth spatial dimension denoted as \hat{w} are highlighted with light blue. As we can see, the A_{γ_4} is the product of 32 σ^x operators on the 32 links of a 4-dimensional hypercube.

C. Review of GSD Computation

In this subsection, we give a brief review of some GSD computation methods of fracton order systems.

In exactly solvable lattice models of the form $H = \sum_i \mathcal{O}_i$, where every \mathcal{O}_i commutes with each other. By recognizing the ground states of such a model as a stabilizer code with the stabilizer set $\{\mathcal{O}_i\}$, we can find the GSD by counting the number of independent constraints on the stabilizers[3]. While from another perspective, sometimes a complete set of conserved quantities under the stabilizers is obvious to find, then we can obtain the GSD by counting different combinations of conserved numbers[104]. Since from the view of stabilizer codes, the conserved numbers can be regarded as values of logical qubits, the number of logical qubits is just given by $\log_2 GSD$. Therefore, the GSD can also be computed by counting logical operators. These logical operators flip logical qubits.

For instance, let's consider the 2D toric code model, where qubits are defined on the links of a square lattice

with periodic boundary condition. The Hamiltonian is defined as follows:

$$H_{TC} = -J \sum_p A_p - K \sum_v B_v, \quad (8)$$

where coupling constants $J, K > 0$, $A_p = \prod_{i \in p} \sigma_i^x$, $B_v = \prod_{j \in v} \sigma_j^z$. Here p refers to plaquette, and v refers to vertex. By counting independent constraints over stabilizers A_p 's and B_v 's, we can obtain that $\dim(\mathcal{H}_{logical}) = 2^2 = 4$. That is to say, the ground state is 4-fold degenerated[3]. Here $\mathcal{H}_{logical}$ refers to the Hilbert space spanned by the logical qubits.

By the conserved number counting method, we can see that in the σ^z basis, the logical operators are given by $W(l) = \prod_{i \in l} \sigma_i^x$, where l is a non-contractable loop composed of links of the lattice. As there are only two such operators which are independent to each other, we can see there are $2^2 = 4$ possible combinations of the values of the logical qubits. As a result, the GSD is 4[104].

Recently, a polynomial representation of translational invariant commuting Hamiltonians is proposed[6, 7, 59]. This representation gives a general method to calculate the GSD of a large class of models. While in foliated fracton topological orders[10, 11, 24, 25, 56, 58, 75], there is a special way to count the logical operators in the ground states. Due to the existence of the foliation structure, the GSD of a foliated fracton order can be obtained by taking the product of the GSD of the topological orders on the leaves with certain corrections. Ref. [11] demonstrated this method by computing the GSD of X-cube model on a 3-torus with this counting method, where the result is consistent with the algebraic algorithm proposed in Ref. [6].

Besides, since it has been found that the ground states of some fracton models can be described by corresponding variations of TQFT, the GSD of these models can also be reproduced in the field theories. See Ref. [19, 26, 39] for some examples.

III. GSD OF $[d_n, d_s, d_l, D]$ MODELS

A. Representing Ground States with Low Dimensional Data

As we're trying to compute the GSD of a $[d_n, d_s, d_l, D]$ model by data from lower dimensional subsystems², it is important to define the subsystem structures strictly. So in this subsection, we will introduce the definition of decomposition and restriction of lattices, spin configurations and ground states. And finally, we prove that when

² In this paper, we use "sublattice" and "subsystem" alternatively.

$d_s - d_n = 1$, there is a one-to-one correspondence between a collection of SGSs satisfying certain *consistent conditions* (to be defined in this section) and a ground state of the original system. Consequently, it is plausible to compute the GSD of a $[d_n, d_s, d_l, D]$ model with $d_s - d_n = 1$ by counting the number of possible combinations of subsystem states. As $d_s - d_n = 1$ is necessary for the decomposition of ground states, it is always assumed in the following part of this section.

1. Decomposition of Lattices

To define a decomposition of a ground state in a general $[d_n, d_s, d_l, D]$ model, we find that it is convenient to consider a decomposition of manifolds. In some higher dimensional models, we can consider “leaves of a leaf”, as the “ground state degeneracy” of a leaf can also be subextensive. From another view, a high dimensional $[d_n, d_s, d_l, D]$ model may admit foliation structures of various dimensions. As a result, we believe it is beneficial to define a “decomposition” of the base manifold. Besides, in this paper, as we are mainly interested in lattice models, manifolds are always assumed to be equipped with a lattice structure (i.e. cellulation) given by the definition of a $[d_n, d_s, d_l, D]$ model. Therefore, when the lattice structure is specified, we will alternatively use “lattice” and “manifold”. For simplicity, in the paper we only consider toric base manifolds.

For a base manifold M^D , we define a (d_1, d_2, \dots, d_k) -decomposition as a collection composed of sets of lower dimensional manifolds

$$\mathcal{M} \equiv \{M^{d_1}\} \cup \{M^{d_2}\} \cup \dots \cup \{M^{d_k}\}, \quad (9)$$

which satisfies that (without loss of generality, we always assume $d_1 < d_2 < \dots < d_k$):

- For any $\{M^{d_i}\}$, we have $\cup_{M \in \{M^{d_i}\}} M = M^D$. Specially, for lattices, this condition requires every qubit to belong to at least one sublattice $M \in \{M^{d_i}\}, \forall d_i$.
- For any pair of sets of lower dimensional manifolds $\{M^{d_i}\}$ and $\{M^{d_j}\}$ with $d_i < d_j$, we require that for any $M^{d_j} \in \{M^{d_j}\}$, there exists a subset $\{\tilde{M}^{d_i}\} \subset \{M^{d_i}\}$, such that $\cup_{M^{d_i} \in \{\tilde{M}^{d_i}\}} M^{d_i} = M^{d_j}$. For lattices, this condition requires every qubit in M^{d_j} to belong to at least one sublattice $M^{d_i} \in \{\tilde{M}^{d_i}\}$.
- $M_1^{d_i} \cap M_2^{d_i}$ can only be a $(d_i - 1)$ -dimensional sublattice or empty set.

Here, please note that these conditions show that a decomposition of a manifold equipped with a lattice structure can only be determined when the $[d_n, d_s, d_l, D]$ model is specified. When the collection contains only subsystems (i.e. M^{d_i} with $d_i < D$) of the same dimension, it restores to a regular foliation of M^D [102]. While

when the collection contains sets of sublattices of different dimensions, the decomposition gives all higher dimensional sublattices foliation structures, too (see Fig. 2).

In this paper, as we don't discuss about the influence of the topology of sublattices in detail, we always assume that the decompositions are composed of toric sublattices.

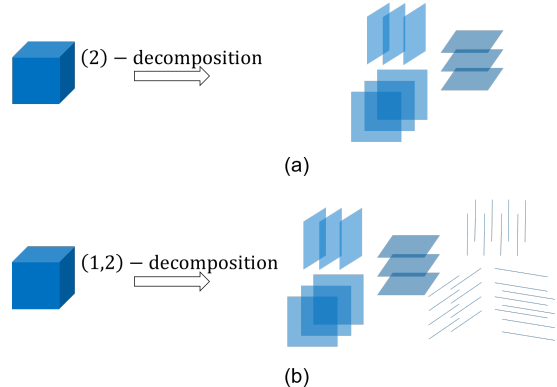


FIG. 2. Different decompositions of 3-torus for X-cube model, where spins are located on links. As we can see, while the decomposition in (a) shows a regular 2-dimensional foliation of the original 3-manifold, the decomposition in (b) additionally gives a foliation structure to each 2-dimensional leaf space in (a).

2. Decomposition of Configurations and Operators

Next, for a given decomposition \mathcal{M} of the base manifold M^D , we can define the decomposition of Ising configurations and operators. While at first, it would be more convenient to define the restriction of such structures on sublattices. Without special note, in this paper we only consider $\frac{1}{2}$ -spins as basic degrees of freedom, and the σ^z basis is always assumed.

Given a model defined on M^D and one of its decomposition \mathcal{M} , when there is an inclusion $I : M_i^{d_1} \hookrightarrow M_j^{d_2}$, we can define the restriction of an arbitrary spin configuration: $[\rho^c]_{M_i^{d_1}}^{M_j^{d_2}}(c_{M_j^{d_2}}) = c_{M_i^{d_1}}$. It maps $c_{M_j^{d_2}}$ to $c_{M_i^{d_1}}$ by simply dropping all degrees of freedom out of $M_i^{d_1}$. Here, $c_{M_i^{d_1}}$ and $c_{M_j^{d_2}}$ are configurations respectively defined on $M_i^{d_1}$ and $M_j^{d_2}$, and the superscript c stands for “configuration”. Then, for a given configuration c and manifold decomposition \mathcal{M} , we can define the decomposition of the configuration c on \mathcal{M} as $\Omega_{\mathcal{M}}^c(c)$, by taking the set of all restrictions of c on sublattices inside \mathcal{M} . That is to say, we have

$$\Omega_{\mathcal{M}}^c(c) \equiv \{c_{M^{d_1}}\} \cup \{c_{M^{d_2}}\} \cup \dots \cup \{c_{M^{d_k}}\}, \quad (10)$$

where $c_{M^{d_i}}$ refers to the restriction of the Ising configuration c on a d_i -dimensional sublattice M^{d_i} . According

to the definition of \mathcal{M} , the original configuration c can be reconstructed from one of its decomposition $\Omega_{\mathcal{M}}^c(c)$. A pictorial demonstration of the restriction of configurations is given in Fig. 3.

Similarly, with a given model and a decomposition \mathcal{M} , for a class of specially interesting operators, o composed of σ^x operators (dubbed as an X -operator for simplicity), we can also define their restriction and decomposition. When there is an inclusion $I : M_i^{d_1} \hookrightarrow M_j^{d_2}$, the restriction $[\rho^o]_{M_i^{d_1}}^{M_j^{d_2}}(o_{M_j^{d_2}}) = o_{M_i^{d_1}}$ maps an X -operator totally supported on $M_j^{d_2}$ to an X -operator totally supported on $M_i^{d_1}$, by dropping all σ^x operators defined on γ_{d_s} 's out of $M_i^{d_1}$. Here the superscript o stands for ‘‘operator’’. Again, for a given X -operator o and manifold decomposition \mathcal{M} , we can define the decomposition of the X -operator o on \mathcal{M} as $\Omega_{\mathcal{M}}^o(o)$, by taking the set of all restrictions of o on sublattices inside \mathcal{M} . That is to say, we have

$$\Omega_{\mathcal{M}}^o(c) \equiv \{o_{M^{d_1}}\} \cup \{o_{M^{d_2}}\} \cup \dots \cup \{o_{M^{d_k}}\}, \quad (11)$$

where $o_{M^{d_i}}$ refers to the restriction of the X -operator o on a d_i -dimensional sublattice M^{d_i} . Since all X -operators commute with each other, an arbitrary X -operator o can also be reconstructed from one of its decomposition $\Omega_{\mathcal{M}}^o(o)$.

3. Decomposition of Ground State Sectors

Then, we can define the decomposition of a ground state sector with a given manifold decomposition \mathcal{M} ³. Nevertheless, this time we have to at first consider how to define a ground state on a sublattice, as it is not as intuitive as the restriction of a configuration. To solve this problem, we need to utilize the properties of ground states of $[d_n, d_s, d_l, D]$ models. For a ground state $|x\rangle$ of a $[d_n, d_s, d_l, D]$ model, it must satisfy the following conditions:

$$B_{\gamma_{d_n}}^l |x\rangle = |x\rangle, \quad \forall l, \gamma_{d_n}; \quad A_{\gamma_D} |x\rangle = |x\rangle, \quad \forall \gamma_D. \quad (12)$$

In σ^z basis, the constraints given by $B_{\gamma_{d_n}}^l$ terms can be realized by requiring that all configurations in $|x\rangle$ satisfy certain conditions. And we use the notation \tilde{c} to refer to such a configuration. As an example, in X-cube model denoted as $[0, 1, 2, 3]$, the B constraint requires that all \tilde{c} 's can only contain strings with trivalent vertices. While the constraints given by A terms require that, for all configurations which can be transformed to each other by

applying A_{γ_D} operators, they must be equally superpositioned in a ground state $|x\rangle$. Consequently, a ground state $|x\rangle$ of a $[d_n, d_s, d_l, D]$ model can be regarded as a set of configuration c 's, and the set satisfies constraints given by both A and B terms. Similarly, a subsystem ground state sector (SGS) on sublattice M^{d_i} denoted as $x_{M^{d_i}}$, can be defined as a set of $c_{M^{d_i}}$, which satisfies the following conditions:

- An SGS $x_{M^{d_i}}$ contains only $\tilde{c}_{M^{d_i}}$. $\tilde{c}_{M^{d_i}}$ is a $c_{M^{d_i}}$ that can be obtained as the restriction of a \tilde{c} on M^{d_i} . This condition is resulted from the B constraint over original ground states.
- Two $\tilde{c}_{M^{d_i}}$'s belong to the same $x_{M^{d_i}}$ if and only if they can be connected under the action of $[\rho^o]_{M^{d_i}}^{M^D}(A_{\gamma_D})$. This condition is resulted from the A constraint over original ground states.

Now we can see that, according to our definition of SGSs, there is a well-defined restriction of a ground state x ⁴: $[\rho^x]_{M_i^{d_1}}^{M^D}(x) = x_{M_i^{d_1}}$, which maps a ground state to an SGS on $M_i^{d_1}$ (to see the existence of this map, we only need to notice that by definition, the restriction of A_{γ_D} operators doesn't change subsystem ground state sectors). Then we can define the decomposition of a ground state x on \mathcal{M} following exactly the same manner as configurations and X -operators, by taking the set of all restrictions of x on sublattices inside \mathcal{M} . So we have

$$\Omega_{\mathcal{M}}^x(x) \equiv \{x_{M^{d_1}}\} \cup \{x_{M^{d_2}}\} \cup \dots \cup \{x_{M^{d_k}}\}, \quad (13)$$

where $x_{M^{d_i}}$ refers to the restriction of the ground state x on a d_i -dimensional sublattice M^{d_i} .

Finally, we prove that a ground state x of a $[d_n, d_s, d_l, D]$ model can also be reconstructed from a decomposition of x on \mathcal{M} , given that (a) \mathcal{M} contains $(d_s + 1)$ -dimensional subsystems, and (b) $d_s - d_n = 1$. In the following proof, we will show why these two conditions are necessary. We only need to prove that given \mathcal{M} includes $\{M^{d_s+1}\}$ and $d_s - d_n = 1$, for $x_1 \neq x_2$, we have $\Omega_{\mathcal{M}}^x(x_1) \neq \Omega_{\mathcal{M}}^x(x_2)$.

Proof. We use contradiction to prove it. For a given \mathcal{M} including $\{M^{d_s+1}\}$, we assume that there exists a pair of ground states $x_1 \neq x_2$, such that $\Omega_{\mathcal{M}}^x(x_1) = \Omega_{\mathcal{M}}^x(x_2)$. As x_1 and x_2 are different ground states, they can always be connected by a logical operator denoted as o_x . So we have $o_x |x_1\rangle = |x_2\rangle$. In a $[d_n, d_s, d_l, D]$ model, when $d_s - d_n = 1$, logical operators are always generated by $W(S^{d_s}) = \prod_{\gamma_{d_s} \in S^{d_s}} \sigma_{\gamma_{d_s}}^x$. These logical operators are composed of σ^x operators along non-contractable S^{d_s} 's. Nevertheless, not all such $W(S^{d_s})$ logical operators are independent to each other. The product of $W(S^{d_s})$'s

³ We use ‘‘ground state sectors’’ instead of ‘‘ground states’’ in this section to emphasize that they can be regarded as sets of configurations, as demonstrated in this subsection

⁴ To stress that x is a set here, we omit the bracket notation

where all S^{d_s} 's compose the d_s -dimensional boundary of a non-contractable S_D (i.e. S_D is extended along at least one dimension), becomes the trivial logical operator, as such a product can be written as a product of A_{γ_D} operators. Therefore, we can see that there must be a $(d_s + 1)$ -dimensional subsystem $M_1^{d_s+1}$ in \mathcal{M} , where the restriction of o_x is a $W(S^{d_s})$ operator, which flips all spins along an S^{d_s} . Such an operator changes the SGS on $M_1^{d_s+1}$, as it cannot be a product of restrictions of A_{γ_D} operators on $M_1^{d_s+1}$, and it is against our assumption. Thereupon, the map from ground states to collections of subsystem ground state sectors is an injection. So a ground state x of a $[d_n, d_s, d_l, D]$ model can be reconstructed from its decomposition on \mathcal{M} . \square

In the rest part of this section, for $[d_n, d_s, d_l, D]$ models, we always assume that our manifold decompositions contain $(d_s + 1)$ -dimensional subsystems and $d_s - d_n = 1$, such that we can faithfully decompose ground states. Furthermore, if we only consider the collections of SGSs which are decompositions of original ground states, we can see that there is an isomorphism between ground states and such collections of subsystem ground state sectors. The condition that a collection of SGSs has to satisfy such that it can be obtained by decomposing an original ground state, is dubbed as the *consistent condition*.

In summary, once we've found the SGSs of a decomposition and their consistent conditions, the ground state degeneracy can be obtained by counting the number of consistent combinations of SGSs. Nevertheless, here we need to notice that usually the consistent conditions cannot be systematically derived.

As an example, let us consider the ordinary (2)-decomposition (i.e. 2-dimensional foliation) of X-cube model[25]. The B constraints of configurations is that all \tilde{c} 's can only have trivalent vertices. On 2-dimensional subsystems, this constraint requires all \tilde{c}_{M^2} 's in an SGS are closed string configurations. And the restriction of A_{γ_3} stabilizers on 2-dimensional subsystems are just plaquette operators $A_{\gamma_2} \equiv \sigma_{\gamma_1^1}^x \sigma_{\gamma_1^2}^x \sigma_{\gamma_1^3}^x \sigma_{\gamma_1^4}^x$, where $\gamma_1^1, \gamma_1^2, \gamma_1^3, \gamma_1^4$ are four links of a certain plaquette γ_2 . That is to say, we have $[\rho^o]_{M_i^2}^{M^3}(A_{\gamma_3}) = A_{\gamma_2}$. As a result, an X-cube ground state can be determined by a consistent collection of 2D SGSs, where an SGS can be identified as a 2D toric code ground state. The consistent condition here is given in Sec. III C. Besides, a detailed demonstration of how to obtain the GSD of X-cube model by counting consistent collections is also given in Sec. III C.

B. General Procedures of the Calculation

Before the concrete calculation, we believe it is beneficial to give a brief introduction of the key steps of the calculation.

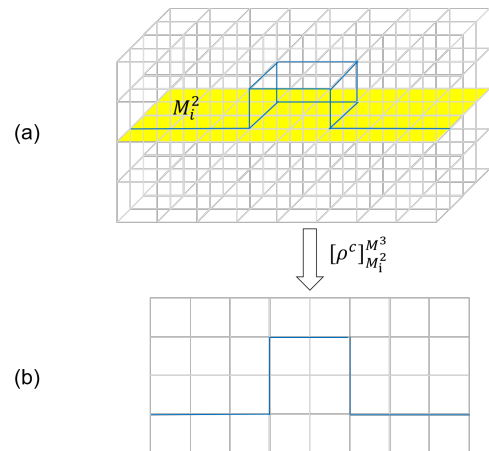


FIG. 3. Restriction of configurations in X-cube model. (b) demonstrates the restriction of the blue string composed of flipped spins on subsystem M_i^2 . M_i^2 is the plane highlighted with yellow in (a).

For $[0, 1, 2, D]$ and $[D-3, D-2, D-1, D]$ models, they all have decompositions where all SGSs of a certain dimension can be identified as ground state sectors of some pure topological orders. That is to say, these SGSs can be obtained by exactly the same manner as in some pure topological ordered models. Once we've found the SGSs by logical operator counting, we can use a combinatorial way to deal with the calculation of GSD of the original FTO models. Generally, the calculation is composed of 3 parts: firstly, we extract a characteristic graph from the model, which can encode all possibilities combinations of logical operators in a pictorial manner. Then, we construct a coloring problem based on the characteristic graph. And finally, we solve this coloring problem in an algebraic way.

Since the calculation sounds kind of circuitous, in the next section, we will at first use this method to calculate the GSD of X-cube model, to provide an intuitive picture of the method. Sec. III D demonstrates the calculation of the GSD of $[0, 1, 2, D]$ models and $[D-3, D-2, D-1, D]$ models (here D is the spatial dimension of the model). Our results for X-cube ($[0, 1, 2, 3]$) model are consistent with the results given by other methods[7, 11]. In the end, we give a brief discussion about a mathematical interpretation of our results.

C. Computation of the GSD of X-cube Model as a Coloring Problem

We begin with an introduction of the ground states of X-cube model (for a more detailed review of X-cube model, see Ref. [4, 5]).

Similar to toric code model, independent ground states of X-cube model can be distinguished by the action of non-local logical operator $W(S^1) = \prod_{l \in S^1} \sigma_l^x$ with different S^1 . Therefore, the GSD of X-cube model can be

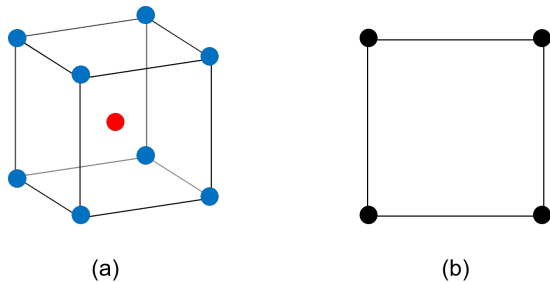


FIG. 4. A simple pictorial demonstration of the X-cube model. In (a), the red dot at the center of the cube represents the A_c term in the hamiltonian, while the blue dots represent the B_i^z terms. (b) is the characteristic graph of X-cube model defined on a $2 \times 2 \times 2$ cubic lattice with periodic boundary condition.

calculated by counting the number of inequivalent combinations of non-local logical operators $W(S^1)$. While unlike in toric code model, where string operators can be moved and deformed arbitrarily, here $W(S^1)$ is strictly supported along an absolutely straight string S^1 . Similar to toric code ground state where two parallel non-local strings can annihilate each other under the action of stabilizers $A_{\gamma_2} = \prod_{i \in \gamma_2} \sigma_i^x$, in X-cube model four strings that compose the 1-dimensional boundary of an S^3 extended in one direction can be annihilated by applying A_c stabilizers. Pictorially, we can say that if 4 strings are exactly the 4 hinges of a quadrangular prism that is extended along the axial direction, then the 4 strings can be created or annihilated by A_c stabilizers. In other words, one single non-local string can be “split” to 3 different non-local strings, as these two string configurations are equally superpositioned in one ground state. This split rule will be utilized in the following sections frequently.

From another perspective, as discussed in Sec. II, here we can consider X-cube ground state sectors as consistent collections of SGSs. For the 3-torus where X-cube model is defined, there are only two possible decompositions, (1, 2)-decomposition and (2)-decomposition. As we can see that in the σ^z basis, for any $M_i^1 \in \{M^1\}$, all $c_{M_i^1}$ can be connected to each other by A_c 's, here we only need to consider the (2)-decomposition $\mathcal{M} = \{M^2\}$ and ignore the discussion about SGSs on M^1 's. For an arbitrary 2D subsystem $M_i^2 \in \{M^2\}$, we can obtain its SGS in the following manner:

- B terms require all $\tilde{c}_{M_i^2}$'s can only contain closed strings;
- A terms require two $\tilde{c}_{M_i^2}$'s belong to the same $x_{M_i^2}$ if and only if they can be connected by $[\rho^0]_{M_i^2}^{M^3}(A_{\gamma_3}) = A_{\gamma_2}$. Here $A_{\gamma_2} \equiv \sigma_{\gamma_1^1}^x \sigma_{\gamma_1^2}^x \sigma_{\gamma_1^3}^x \sigma_{\gamma_1^4}^x$, where $\gamma_1^1, \gamma_1^2, \gamma_1^3, \gamma_1^4$ are four links of a certain plaquette γ_2 .

By noticing that A_{γ_2} is equivalent to the plaquette term in 2D toric code model, and the constraint given

by B term is the same as the vertex term in 2D toric code model, we can see the SGSs on M_i^2 is exactly the same as the ground states of 2D toric code model. That is to say, on any M_i^2 , SGSs are also determined by the parity of number of non-local σ^x -strings (i.e. logical operators) along the two perpendicular directions as in 2D toric code model. From direct observation, here the consistent condition between SGSs can also be found: parity of the number of non-local strings along the same direction must be altered on two perpendicular M^2 's simultaneously. Under this condition, the “split rule” of X-cube ground state sectors is reproduced exactly. Therefore, we can calculate the GSD of X-cube model by simply counting the number of consistent combinations of toric code ground state sectors on 2D subsystems. Namely, the GSD of X-cube model can be obtained by counting all possible combinations of inequivalent non-contractable loops on 2D subsystems.

To solve this counting problem, firstly, we notice that the non-contractable loops in an X-cube ground state can be classified into 3 independent sets, according to their directions. Loops along different axes contribute to the ground state independently. Therefore, a ground state of X-cube model is determined by 3 identical independent parts, and to compute the GSD of an X-cube model, we only need to consider the number of possible combinations of loops of one part, and the total GSD is just the cube of it.

Without loss of generality, let's consider the non-contractable loops along \hat{x} -axis only. Such loops only influence the parity of number of loops along \hat{x} -axis in $\langle \hat{x}\hat{y} \rangle$ - and $\langle \hat{x}\hat{z} \rangle$ -leaves. Therefore, we can draw a “characteristic graph” for such a part. A characteristic graph looks like a $\langle \hat{y}\hat{z} \rangle$ -leaf, while the vertices refer to the lines along the \hat{x} -axis in the original lattice, and the lines in the graph refer to $\langle \hat{x}\hat{y} \rangle$ - and $\langle \hat{x}\hat{z} \rangle$ -leaves (Fig. 4 gives an example of a characteristic graph). Naturally, leaves intersecting at a line are represented by lines intersecting at the corresponding vertex in the characteristic graph.

With the characteristic graphs defined above, the GSD computation can be converted to a coloring problem. The existence of a non-contractable loop along \hat{x} -axis can be recognized as “coloring” of a vertex in the characteristic graph, and the corresponding change of parity of number of loops on the associated leaves, can be recognized as the coloring of the lines that intersect at the colored vertex (i.e. coloring of all edges along the line). Fig. 5 shows a simple example of this correspondence. Consequently, our original question, which aims to find all possible combinations of the parity of number of loops along \hat{x} -axis in $\langle \hat{x}\hat{y} \rangle$ - and $\langle \hat{x}\hat{z} \rangle$ -leaves, is converted to finding all possible edge-coloring patterns⁵ in the characteristic graph.

⁵ As all edges along the same lines are always colored the same way, for characteristic graphs we can use “edge” and “line” alternatively.

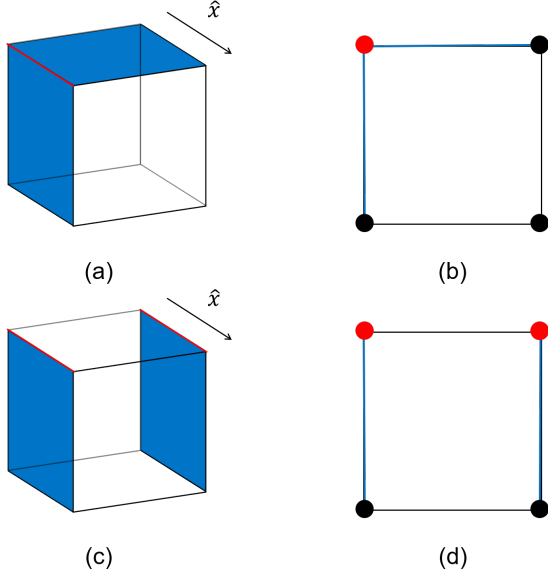


FIG. 5. An example of the correspondence between a configuration with non-contractable loops in X-cube model and the associated characteristic graph. The red line in (a) refers to a non-contractable loop, and the leaves with flipped parity are highlighted with blue. In (b), the vertex corresponding to the line with a non-contractable loop is colored with red, and its associated lines are colored with blue. In (c), we add another non-contractable loop that is parallel to the first one. Then, since the parity of the top leaf has been flipped twice, it restores to the uncolored state, and in its corresponding coloring pattern of characteristic map (d), the line represents the top leaf is also uncolored.

Finally, in order to count the number of possible edge coloring patterns, we introduce a “characteristic group” based on following rules:

- All edge-coloring patterns of characteristic graphs that can be realized by vertex coloring are recognized as group elements.
- A vertex in the characteristic graph corresponds to a generator of the group, which is the edge-coloring pattern obtained by coloring all lines that intersect at the vertex. Different vertex corresponds to different generators.
- The multiplication of two elements is the pattern generated by the product of the generators that generate the original two elements. Due to the physical meaning of the coloring, we can see the multiplication is equivalent to \mathbb{Z}_2 addition of coloring of lines.
- Every generator defined above is its own inverse element.
- The product of four generators whose corresponding vertices form a rectangle equals to the identity element (i.e. the no-coloring pattern). This rule

corresponds to the split rule discussed in the previous part of this section.

As the identity elements and inverse elements are already given in the above rules, we only need to check whether the above defined structure is closed and associative. According to our definition of the multiplication, all multiplication results can be generated by vertex colorings, so the structure is closed. And since the multiplication is equivalent to the \mathbb{Z}_2 addition of coloring of lines, the multiplication is associative and commutative. Therefore, we can see that the structure is indeed an Abelian group.

As a result, we can simply find the number of different patterns by calculating the number of group elements.

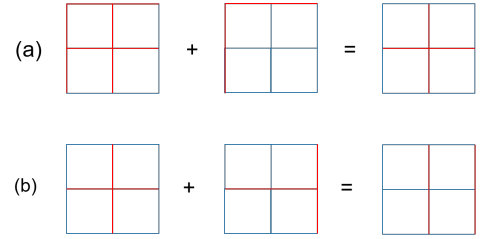


FIG. 6. Examples of the multiplication of edge-coloring patterns. Here we only draw the 3×3 size cases. We didn’t present the vertex elements that generate the patterns since a pattern can be generated by different combinations of vertex elements.

If we ignore the constraints given by the split rule, the group should be a direct product of $L^2 \mathbb{Z}_2$ groups (L is the linear size of the lattice and the characteristic graph). While under the constraints, we notice that since the constraints are not all independent from each other, only $(L - 1)^2$ constraints that correspond to the plaquettes in the characteristic graph are necessary to generate all constraints. We can use each independent constraint to eliminate one generator in a plaquette. At last, only $L^2 - (L - 1)^2 = 2L - 1$ independent \mathbb{Z}_2 degrees of freedom remain, so the group has 2^{2L-1} elements in total (Fig. 7 gives a pictorial demonstration of the elimination of degrees of freedom). Therefore, the ground state degeneracy of a X-cube model defined on a lattice of the size $L \times L \times L$ with periodic boundary condition should be $(2^{2L-1})^3 = 2^{6L-3}$ (since we’ve dismantled the model into 3 independent parts), that is to say, we have $\log_2 GSD = 6L - 3$, which is consistent with the known result[25].

Though the process of this calculation seems to be a little circuitous, in the next section, we will see it is really powerful for computing some more complicated cases.

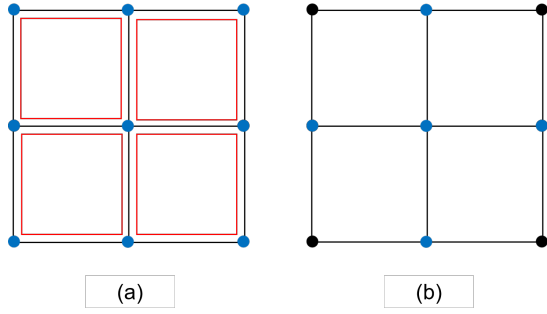


FIG. 7. Pictorial Demonstration of the Elimination of Additional Degrees of Freedom in the Characteristic Graphs. The red squares in (a) represent the independent constraints associated with plaquettes, and the blue vertices represent the generators. In (b), since each independent constraint makes one generator in a plaquette redundant, we can simultaneously forget the redundant generators and the constraints to get 5 independent degrees of freedom.

D. GSD of $[0, 1, 2, D]$ and $[D - 3, D - 2, D - 1, D]$ Models

1. Isotropic Lattice

In this subsection, we will calculate the GSD of $[0, 1, 2, D]$ and $[D - 3, D - 2, D - 1, D]$ models with $D \geq 4$. Before the concrete calculation, we would like to make some brief remarks to demonstrate how to construct the calculation for such models.

- For a $[0, 1, 2, D]$ model, its $(D - 1)$ -dimensional SGSs can be found to be equivalent to the ground state sectors of $[0, 1, 2, D - 1]$ model, following the same logic as in Sec. III C. By decomposing the ground state sectors recursively, we find that in order to calculate the GSD of a $[0, 1, 2, D]$ model, we only need to consider the $(d_s + 1)$ -decomposition (as in σ_z basis, all configurations on d_s -dimensional subsystems can be connected by the action of A_{γ_D} , SGSs on M^{d_s} 's contains no information of the original ground state, so they can be ignored in the calculation of GSD). As a result, for a $[0, 1, 2, D]$ model we can obtain its GSD by merely considering its 2-dimensional SGSs and their consistent conditions.
- Following the same logic as for X-cube model, since logical operators of the form $\prod_{\gamma_{d_s} \in S^{d_s}} \sigma_{\gamma_{d_s}}^x$ with non-contractable S^{d_s} generate all inequivalent SGSs for $[0, 1, 2, D]$ and $[D - 3, D - 2, D - 1, D]$ models, a ground state sector is also determined by the parity of number of flipped S^{d_s} along different directions. Again, by direct observation we can see that the consistent condition of SGSs is that the parity of number of S^{d_s} along the same direction in $(D - d_s)$ intersecting subsystems must be altered simultaneously. Then, we can see that the charac-

teristic graph method in Sec. III C also applies to more general $[d_n, d_s, d_l, D]$ models.

- it is easy to see that the number of normal directions for S^{d_s} in the whole system is just $\binom{D}{d_s}$, so we can decompose the whole system to $\binom{D}{d_s}$ parts. Besides, since a characteristic graph is obtained by simply regarding d_s -dimensional subsystems as vertices, the characteristic graph of a $[0, 1, 2, D]$ or $[D - 3, D - 2, D - 1, D]$ model should be $(D - d_s)$ -dimensional. The lines in a characteristic graph still refer to d_l -dimensional subsystems. Again, we can obtain a split rule, that coloring all vertices of a $(D - d_s)$ -dimensional hypercuboid keeps the edge coloring pattern unchanged. Therefore, we have almost the same rule as in X-cube model for mapping the coloring problem on the characteristic graph to the characteristic group: vertices for generators, and $\gamma_{D-d_s} s'$ for independent constraints.

In summary, for a $[0, 1, 2, D]$ (where $d_2 = 2$) or $[D - 3, D - 2, D - 1, D]$ (where $d_s = D - 2$) model, we have a $(D - d_s)$ -dimensional characteristic graph, whose vertices correspond to generators while $\gamma_{D-d_s} s'$ correspond to independent constraints of the characteristic group. And again, based on the one-to-one correspondence between inequivalent ground states and different coloring patterns, we have $\log_2 GSD = \binom{D}{d_s} \times (L^{D-d_s} - (L-1)^{D-d_s})$.

Therefore, for $[0, 1, 2, D]$ models, we have $\log_2 GSD = D \times (L^{D-1} - (L-1)^{D-1}) = D \times \sum_{n=0}^{D-2} \binom{D-1}{n} (-1)^{D+n} L^n$. When $D = 3$, the result will be reduced to the X-cube case.

And for $[D - 3, D - 2, D - 1, D]$ models, we have $\log_2 GSD = \binom{D}{D-2} \times (L^2 - (L-1)^2) = \binom{D}{D-2} \times (2L-1) = (D^2 - D) \times L - \frac{D^2 - D}{2}$. Again, when $D = 3$, the result will be reduced to the X-cube case.

2. Anisotropic Lattice

According to the construction of our method, we can see it can be rather simply generalized to anisotropic lattices, by adjusting the size of characteristic graphs.

As an example, for a $[0, 1, 2, D]$ model defined on a lattice of the size $L_1 \times L_2 \times L_3 \times \dots \times L_D$, the D characteristic graphs of the model are respectively of the size $L_2 \times L_3 \times \dots \times L_D$, $L_1 \times L_3 \times \dots \times L_D$, \dots , and $L_1 \times L_2 \times L_3 \times \dots \times L_{D-1}$. Each of the characteristic graphs contributes a $(\frac{1}{L_j} \prod_i^D L_i) - (\frac{1}{L_j-1} \prod_i^D (L_i - 1))$

term to the $\log_2 GSD$, so the GSD is given by:

$$\begin{aligned}
\log_2 GSD &= \sum_j^D \left\{ \left(\frac{1}{L_j} \prod_i^D L_i \right) - \left(\frac{1}{L_j - 1} \prod_i^D (L_i - 1) \right) \right\} \\
&= 2 \times \left(\sum_{k_1}^D \sum_{k_2}^{k_1-1} \frac{1}{L_{k_1} L_{k_2}} \prod_n L_n \right) \\
&\quad - 3 \times \left(\sum_{k_1}^D \sum_{k_2}^{k_1-1} \sum_{k_3}^{k_2-1} \frac{1}{L_{k_1} L_{k_2} L_{k_3}} \prod_n L_n \right) \\
&\quad + 4 \times \left(\sum_{k_1}^D \sum_{k_2}^{k_1-1} \sum_{k_3}^{k_2-1} \sum_{k_4}^{k_3-1} \frac{1}{L_{k_1} L_{k_2} L_{k_3} L_{k_4}} \prod_n L_n \right) \\
&\quad + \dots \\
&\quad + (-1)^{D-1} (D-1) \sum_n^D L_n.
\end{aligned}$$

Similarly, for a $[D-3, D-2, D-1, D]$ model defined on a lattice of the size $L_1 \times L_2 \times L_3 \times \dots \times L_D$, we have

$$\begin{aligned}
\log_2 GSD &= \sum_i^D \sum_j^{i-1} \{L_i \times L_j - (L_i - 1) \times (L_j - 1)\} \\
&= \sum_i^D \sum_j^{i-1} \{L_i + L_j - 1\} \\
&= \sum_i^D (D-1) \times L_i - \frac{D^2 - D}{2}.
\end{aligned}$$

E. Remarks about GSD

Compare the GSD of X-cube, $[0, 1, 2, D]$ and $[D-3, D-2, D-1, D]$ models, we have the following observations:

- In a $[0, 1, 2, D]$ model, the $\log_2 GSD$ becomes a polynomial. Such a polynomial contains not only the linear and constant terms, but also terms of any degrees that smaller than $D-1$.
- In a $[D-3, D-2, D-1, D]$ model, the $\log_2 GSD$ is of same form as X-cube model.

The polynomial $\log_2 GSD$ in $[0, 1, 2, D]$ models are the most interesting and unprecedented result here. Considering that in a $[0, 1, 2, D]$ model with $D \geq 4$, when the whole system is in a ground state, the state in a $(D-1)$ -dimensional subsystem also looks like a ground state of a fracton model (more exactly, it looks like a ground state of a $[0, 1, 2, D-1]$ model). In some sense, it means the system admits not only a foliation structure, but a multi-level foliation structure, as discussed in Sec. I. And the GSD contains the information of such multi-level foliation, or just decomposition. Mathematically, since we've already known the relation between the

coefficients in the $\log_2 GSD$ of X-cube model and the 2-foliation of the manifold where the system is defined[25], an interesting question is to find the counterpart of such relationship between fracton orders and mathematics in general $[0, 1, 2, D-1]$ models.

From another perspective, we can see that the relation between $[0, 1, 2, 4]$ and X-cube model is similar to the relation between X-cube and 2D toric code model. It makes $[0, 1, 2, 4]$ model kind of a ‘‘fracton order of fracton order’’. Such an observation makes us believe that better knowledge about the relation between higher dimensional fracton orders and 3D fracton orders may be beneficial to gain deeper insights about the nature of fracton orders.

Last but not least, though we've restricted our discussion to models with $d_s - d_n = 1$, there are still a large subset of $[d_n, d_s, d_l, D]$ models worth exploring, such as $[1, 2, 3, 5]$ and $[1, 2, 5, 6]$ models.

IV. CONCLUSION

In this paper, we calculate the GSD of $[d_n, d_s, d_l, D]$ models[71] with a combinatorial method. And to our surprise, a series of polynomials of system sizes are obtained as $\log_2 GSD$, as summarized in Table. I. These coefficients are expected to reflect a series of topological and geometric properties of the models. Therefore, it seems to be a non-trivial question to give a further exploration of the physical and mathematical origins of these polynomials. Besides, the mathematical interpretation of the coefficients of the terms in $\log_2 GSD$ also requires further exploration. These questions may be answered by considering $[d_n, d_s, d_l, D]$ models on general manifolds[25].

In order to compute the GSD, we demonstrate a method to represent a ground state with a collection of lower dimensional data. Then it is a natural question to ask if such low dimensional representations can applied to excitations. Since excitations can have representations as composites of collections of subsystem superselection sectors with the form of $(e m) + (m e)$. Such composites may be recognized as being composed of ‘‘entangled’’ topological excitations. Therefore, we believe the decomposition of excitations may also reveal some interesting features of fracton orders, which will be presented in [105].

ACKNOWLEDGEMENTS

This work was supported in part by the Sun Yat-sen University startup grant, Guangdong Basic and Applied Basic Research Foundation under Grant No. 2020B1515120100, National Natural Science Foundation of China (NSFC) Grant (No. 11847608 & No. 12074438).

-
- [1] Xiao-Gang Wen, *Quantum field theory of many-body systems: from the origin of sound to an origin of light and electrons* (Oxford University Press, 2004).
- [2] Xiao Gang Wen, “A theory of 2+1D bosonic topological orders,” (2016), [arXiv:1506.05768](#).
- [3] A. Yu. Kitaev, “Fault-tolerant quantum computation by anyons,” *Annals of Physics* **303**, 2–30 (2003), [arXiv:quant-ph/9707021 \[quant-ph\]](#).
- [4] Rahul M. Nandkishore and Michael Hermele, “Fractons,” *Annual Review of Condensed Matter Physics* **10**, 295–313 (2019), [arXiv:1803.11196 \[cond-mat.str-el\]](#).
- [5] Michael Pretko, Xie Chen, and Yizhi You, “Fracton phases of matter,” *International Journal of Modern Physics A* **35**, 2030003 (2020), [arXiv:2001.01722 \[cond-mat.str-el\]](#).
- [6] Sagar Vijay, Jeongwan Haah, and Liang Fu, “A new kind of topological quantum order: A dimensional hierarchy of quasiparticles built from stationary excitations,” *Phys. Rev. B* **92**, 235136 (2015).
- [7] Sagar Vijay, Jeongwan Haah, and Liang Fu, “Fracton topological order, generalized lattice gauge theory, and duality,” *Phys. Rev. B* **94**, 235157 (2016).
- [8] Abhinav Prem, Jeongwan Haah, and Rahul Nandkishore, “Glassy quantum dynamics in translation invariant fracton models,” *Physical Review B* (2017), [10.1103/PhysRevB.95.155133](#), [arXiv:1702.02952](#).
- [9] Claudio Chamon, “Quantum glassiness in strongly correlated clean systems: An example of topological overprotection,” *Phys. Rev. Lett.* **94**, 040402 (2005).
- [10] Wilbur Shirley, Kevin Slagle, and Xie Chen, “Foliated fracton order from gauging subsystem symmetries,” *SciPost Phys.* **6**, 41 (2019).
- [11] Han Ma, Ethan Lake, Xie Chen, and Michael Hermele, “Fracton topological order via coupled layers,” *Phys. Rev. B* **95**, 245126 (2017).
- [12] Jeongwan Haah, “Local stabilizer codes in three dimensions without string logical operators,” *Phys. Rev. A* **83**, 042330 (2011).
- [13] Daniel Bulmash and Maissam Barkeshli, “Gauging fractons: Immobile non-Abelian quasiparticles, fractals, and position-dependent degeneracies,” *Phys. Rev. B* **100**, 155146 (2019), [arXiv:1905.05771 \[cond-mat.str-el\]](#).
- [14] Abhinav Prem and Dominic Williamson, “Gauging permutation symmetries as a route to non-Abelian fractons,” *SciPost Physics* **7**, 068 (2019), [arXiv:1905.06309 \[cond-mat.str-el\]](#).
- [15] Daniel Bulmash and Maissam Barkeshli, “Higgs mechanism in higher-rank symmetric U(1) gauge theories,” *Physical Review B* (2018), [10.1103/PhysRevB.97.235112](#), [arXiv:1802.10099](#).
- [16] Kevin T. Tian, Eric Samperton, and Zhenghan Wang, “Haah codes on general three manifolds,” (2018), [arXiv:1812.02101](#).
- [17] Yizhi You, Daniel Litinski, and Felix von Oppen, “Higher-order topological superconductors as generators of quantum codes,” *Phys. Rev. B* **100**, 054513 (2019), [arXiv:1810.10556 \[cond-mat.str-el\]](#).
- [18] Han Ma, Michael Hermele, and Xie Chen, “Fracton topological order from the higgs and partial-confinement mechanisms of rank-two gauge theory,” *Phys. Rev. B* **98**, 035111 (2018).
- [19] Kevin Slagle and Yong Baek Kim, “Quantum field theory of X-cube fracton topological order and robust degeneracy from geometry,” *Physical Review B* **96** (2017), [10.1103/PhysRevB.96.195139](#).
- [20] Gábor B. Halász, Timothy H. Hsieh, and Leon Balents, “Fracton topological phases from strongly coupled spin chains,” *Phys. Rev. Lett.* **119**, 257202 (2017).
- [21] Kevin T. Tian and Zhenghan Wang, “Generalized Haah Codes and Fracton Models,” arXiv e-prints, [arXiv:1902.04543](#) (2019), [arXiv:1902.04543 \[quant-ph\]](#).
- [22] Wilbur Shirley, Kevin Slagle, and Xie Chen, “Foliated fracton order from gauging subsystem symmetries,” *SciPost Phys.* **6**, 41 (2019).
- [23] Wilbur Shirley, Kevin Slagle, and Xie Chen, “Fractional excitations in foliated fracton phases,” *Annals of Physics* **410**, 167922 (2019), [arXiv:1806.08625 \[cond-mat.str-el\]](#).
- [24] Kevin Slagle, David Aasen, and Dominic Williamson, “Foliated field theory and string-membrane-net condensation picture of fracton order,” *SciPost Physics* **6**, 43 (2019).
- [25] Wilbur Shirley, Kevin Slagle, Zhenghan Wang, and Xie Chen, “Fracton models on general three-dimensional manifolds,” *Phys. Rev. X* **8**, 031051 (2018).
- [26] Abhinav Prem, Michael Pretko, and Rahul M. Nandkishore, *Physical Review B*, Tech. Rep. 8 (2018) [arXiv:1709.09673v2](#).
- [27] Shriya Pai, Michael Pretko, and Rahul M. Nandkishore, “Localization in Fractonic Random Circuits,” *Physical Review X* **9**, 021003 (2019), [arXiv:1807.09776](#).
- [28] Shriya Pai and Michael Pretko, “Dynamical Scar States in Driven Fracton Systems,” *Phys. Rev. Lett.* **123**, 136401 (2019), [arXiv:1903.06173 \[cond-mat.stat-mech\]](#).
- [29] Pablo Sala, Tibor Rakovszky, Ruben Verresen, Michael Knap, and Frank Pollmann, “Ergodicity Breaking Arising from Hilbert Space Fragmentation in Dipole-Conserving Hamiltonians,” *Physical Review X* **10**, 011047 (2020), [arXiv:1904.04266 \[cond-mat.str-el\]](#).
- [30] Ajesh Kumar and Andrew C. Potter, “Symmetry-enforced fractonicity and two-dimensional quantum crystal melting,” *Phys. Rev. B* **100**, 045119 (2019).
- [31] Michael Pretko and Leo Radzihovsky, *Physical Review Letters*, Tech. Rep. 19 (2018) [arXiv:1711.11044v2](#).
- [32] Michael Pretko, “Emergent gravity of fractons: Mach’s principle revisited,” *Physical Review D* (2017), [10.1103/PhysRevD.96.024051](#), [arXiv:1702.07613](#).
- [33] Michael Pretko, “Generalized electromagnetism of subdimensional particles: A spin liquid story,” *Phys. Rev. B* **96**, 035119 (2017).
- [34] Leo Radzihovsky and Michael Hermele, “Fractons from Vector Gauge Theory,” *Phys. Rev. Lett.* **124**, 050402 (2020), [arXiv:1905.06951 \[cond-mat.str-el\]](#).
- [35] Arpit Dua, Isaac H. Kim, Meng Cheng, and Dominic J. Williamson, “Sorting topological stabilizer models in three dimensions,” *Phys. Rev. B* **100**, 155137 (2019), [arXiv:1908.08049 \[quant-ph\]](#).
- [36] Andrey Gromov, “Chiral topological elasticity and fracton order,” *Phys. Rev. Lett.* **122**, 076403 (2019).
- [37] Jeongwan Haah, *Lattice quantum codes and exotic topological phases of matter*, Ph.D. thesis, California Institute of Technology (2013).

- [38] Andrey Gromov, “Towards classification of fracton phases: The multipole algebra,” *Phys. Rev. X* **9**, 031035 (2019).
- [39] Yizhi You, Trithep Devakul, S. L. Sondhi, and F. J. Burnell, “Fractonic Chern-Simons and BF theories,” (2019), [arXiv:1904.11530](#).
- [40] John Sous and Michael Pretko, “Fractons from polarons and hole-doped antiferromagnets: Microscopic realizations,” arXiv e-prints , arXiv:1904.08424 (2019), [arXiv:1904.08424 \[cond-mat.str-el\]](#).
- [41] Vedika Khemani, Michael Hermele, and Rahul Nandkishore, “Localization from hilbert space shattering: From theory to physical realizations,” *Phys. Rev. B* **101**, 174204 (2020).
- [42] Juven Wang and Kai Xu, “Higher-Rank Tensor Field Theory of Non-Abelian Fracton and Embeddon,” arXiv e-prints , arXiv:1909.13879 (2019), [arXiv:1909.13879 \[hep-th\]](#).
- [43] Juven Wang and Shing-Tung Yau, “Non-Abelian gauged fracton matter field theory: Sigma models, superfluids, and vortices,” *Physical Review Research* **2**, 043219 (2020), [arXiv:1912.13485 \[cond-mat.str-el\]](#).
- [44] Shriya Pai and Michael Pretko, “Fractonic line excitations: An inroad from three-dimensional elasticity theory,” *Phys. Rev. B* **97**, 235102 (2018).
- [45] Michael Pretko and Rahul M. Nandkishore, “Localization of extended quantum objects,” *Phys. Rev. B* **98**, 134301 (2018).
- [46] Dominic J. Williamson, Zhen Bi, and Meng Cheng, “Fractonic matter in symmetry-enriched $u(1)$ gauge theory,” *Phys. Rev. B* **100**, 125150 (2019).
- [47] Arpit Dua, Dominic J. Williamson, Jeongwan Haah, and Meng Cheng, “Compactifying fracton stabilizer models,” *Phys. Rev. B* **99**, 245135 (2019).
- [48] Bowen Shi and Yuan-Ming Lu, “Deciphering the nonlocal entanglement entropy of fracton topological orders,” *Phys. Rev. B* **97**, 144106 (2018).
- [49] Hao Song, Abhinav Prem, Sheng-Jie Huang, and M. A. Martin-Delgado, “Twisted fracton models in three dimensions,” *Phys. Rev. B* **99**, 155118 (2019).
- [50] Han Ma and Michael Pretko, “Higher-rank deconfined quantum criticality at the lifshitz transition and the exciton bose condensate,” *Phys. Rev. B* **98**, 125105 (2018).
- [51] Juven Wang, Kai Xu, and Shing-Tung Yau, “Higher-Rank Non-Abelian Tensor Field Theory: Higher-Moment or Subdimensional Polynomial Global Symmetry, Algebraic Variety, Noether’s Theorem, and Gauge,” arXiv e-prints , arXiv:1911.01804 (2019), [arXiv:1911.01804 \[hep-th\]](#).
- [52] Kevin Slagle, “Foliated Quantum Field Theory of Fracton Order,” arXiv e-prints , arXiv:2008.03852 (2020), [arXiv:2008.03852 \[hep-th\]](#).
- [53] Dominic J. Williamson and Trithep Devakul, “Type-II fractons from coupled spin chains and layers,” arXiv e-prints , arXiv:2007.07894 (2020), [arXiv:2007.07894 \[cond-mat.str-el\]](#).
- [54] Pranay Gorantla, Ho Tat Lam, Nathan Seiberg, and Shu-Heng Shao, “More Exotic Field Theories in 3+1 Dimensions,” arXiv e-prints , arXiv:2007.04904 (2020), [arXiv:2007.04904 \[cond-mat.str-el\]](#).
- [55] Dung Xuan Nguyen, Andrey Gromov, and Sergej Moroz, “Fracton-elasticity duality of two-dimensional superfluid vortex crystals: defect interactions and quantum melting,” arXiv e-prints , arXiv:2005.12317 (2020), [arXiv:2005.12317 \[cond-mat.quant-gas\]](#).
- [56] Sagar Vijay, “Isotropic Layer Construction and Phase Diagram for Fracton Topological Phases,” arXiv e-prints , arXiv:1701.00762 (2017), [arXiv:1701.00762 \[cond-mat.str-el\]](#).
- [57] Han Ma, A. T. Schmitz, S. A. Parameswaran, Michael Hermele, and Rahul M. Nandkishore, “Topological entanglement entropy of fracton stabilizer codes,” *Phys. Rev. B* **97**, 125101 (2018).
- [58] Wilbur Shirley, Kevin Slagle, and Xie Chen, “Foliated fracton order in the checkerboard model,” (2018), [arXiv:1806.08633](#).
- [59] Jeongwan Haah, “Commuting Pauli Hamiltonians as Maps between Free Modules,” *Communications in Mathematical Physics* **324**, 351–399 (2013).
- [60] Michael Pretko, S. A. Parameswaran, and Michael Hermele, “Odd Fracton Theories, Proximate Orders, and Parton Constructions,” arXiv e-prints , arXiv:2004.14393 (2020), [arXiv:2004.14393 \[cond-mat.str-el\]](#).
- [61] Dominic J. Williamson and Meng Cheng, “Designer non-Abelian fractons from topological layers,” arXiv e-prints , arXiv:2004.07251 (2020), [arXiv:2004.07251 \[cond-mat.str-el\]](#).
- [62] Nathan Seiberg and Shu-Heng Shao, “Exotic \mathbb{Z}_N Symmetries, Duality, and Fractons in 3+1-Dimensional Quantum Field Theory,” arXiv e-prints , arXiv:2004.06115 (2020), [arXiv:2004.06115 \[cond-mat.str-el\]](#).
- [63] David T. Stephen, José Garre-Rubio, Arpit Dua, and Dominic J. Williamson, “Subsystem symmetry enriched topological order in three dimensions,” *Physical Review Research* **2**, 033331 (2020), [arXiv:2004.04181 \[cond-mat.str-el\]](#).
- [64] Nathan Seiberg and Shu-Heng Shao, “Exotic $U(1)$ Symmetries, Duality, and Fractons in 3+1-Dimensional Quantum Field Theory,” *SciPost Phys.* **9**, 46 (2020).
- [65] Andrey Gromov, Andrew Lucas, and Rahul M. Nandkishore, “Fracton hydrodynamics,” *Physical Review Research* **2**, 033124 (2020), [arXiv:2003.09429 \[cond-mat.str-el\]](#).
- [66] Juven Wang, “Non-Liquid Cellular States,” arXiv e-prints , arXiv:2002.12932 (2020), [arXiv:2002.12932 \[cond-mat.str-el\]](#).
- [67] Wilbur Shirley, “Fractonic order and emergent fermionic gauge theory,” arXiv e-prints , arXiv:2002.12026 (2020), [arXiv:2002.12026 \[cond-mat.str-el\]](#).
- [68] David Aasen, Daniel Bulmash, Abhinav Prem, Kevin Slagle, and Dominic J. Williamson, “Topological Defect Networks for Fractons of all Types,” arXiv e-prints , arXiv:2002.05166 (2020), [arXiv:2002.05166 \[cond-mat.str-el\]](#).
- [69] Xiao-Gang Wen, “A systematic construction of gapped non-liquid states,” arXiv e-prints , arXiv:2002.02433 (2020), [arXiv:2002.02433 \[cond-mat.str-el\]](#).
- [70] Ting Fung Jeffrey Poon and Xiong-Jun Liu, “Quantum phase transition of fracton topological orders,” arXiv e-prints , arXiv:2001.05937 (2020), [arXiv:2001.05937 \[cond-mat.str-el\]](#).
- [71] Meng-Yuan Li and Peng Ye, “Fracton physics of spatially extended excitations,” *Phys. Rev. B* **101**, 245134 (2020).

- [72] Jian-Keng Yuan, Shuai A. Chen, and Peng Ye, “Fractonic superfluids,” *Physical Review Research* **2**, 023267 (2020), [arXiv:1911.02876 \[cond-mat.str-el\]](#).
- [73] Shuai A. Chen, Jian-Keng Yuan, and Peng Ye, “Fractonic superfluids (ii): condensing subdimensional particles,” (2020), [arXiv:2010.03261 \[cond-mat.str-el\]](#).
- [74] Hongchao Li and Peng Ye, “Higher Rank Symmetry and Angular Moment Conservation as Emergent Phenomena,” *arXiv e-prints*, [arXiv:2104.03237 \(2021\)](#), [arXiv:2104.03237 \[cond-mat.quant-gas\]](#).
- [75] Wilbur Shirley, Kevin Slagle, and Xie Chen, “Universal entanglement signatures of foliated fracton phases,” *SciPost Phys.* **6**, 15 (2019).
- [76] Tian Lan, Liang Kong, and Xiao-Gang Wen, “Classification of $(3+1)$ D bosonic topological orders: The case when pointlike excitations are all bosons,” *Phys. Rev. X* **8**, 021074 (2018).
- [77] Tian Lan and Xiao-Gang Wen, “Classification of $3+1$ D bosonic topological orders (ii): The case when some pointlike excitations are fermions,” *Phys. Rev. X* **9**, 021005 (2019).
- [78] AtMa P. O. Chan, Peng Ye, and Shinsei Ryu, “Braiding with borromean rings in $(3+1)$ -dimensional spacetime,” *Phys. Rev. Lett.* **121**, 061601 (2018).
- [79] Xueda Wen, Huan He, Apoorv Tiwari, Yunqin Zheng, and Peng Ye, “Entanglement entropy for $(3+1)$ -dimensional topological order with excitations,” *Phys. Rev. B* **97**, 085147 (2018).
- [80] Chenjie Wang and Michael Levin, “Braiding statistics of loop excitations in three dimensions,” *Phys. Rev. Lett.* **113**, 080403 (2014).
- [81] Chao-Ming Jian and Xiao-Liang Qi, “Layer construction of 3d topological states and string braiding statistics,” *Phys. Rev. X* **4**, 041043 (2014).
- [82] Shenghan Jiang, Andrej Mesáros, and Ying Ran, “Generalized modular transformations in $(3+1)$ D topologically ordered phases and triple linking invariant of loop braiding,” *Phys. Rev. X* **4**, 031048 (2014).
- [83] Chenjie Wang, Chien-Hung Lin, and Michael Levin, “Bulk-boundary correspondence for three-dimensional symmetry-protected topological phases,” *Phys. Rev. X* **6**, 021015 (2016).
- [84] Yidun Wan, Juven C. Wang, and Huan He, “Twisted gauge theory model of topological phases in three dimensions,” *Phys. Rev. B* **92**, 045101 (2015).
- [85] Peng Ye, Taylor L. Hughes, Joseph Maciejko, and Eduardo Fradkin, “Composite particle theory of three-dimensional gapped fermionic phases: Fractional topological insulators and charge-loop excitation symmetry,” *Phys. Rev. B* **94**, 115104 (2016).
- [86] Peng Ye and Zheng-Cheng Gu, “Topological quantum field theory of three-dimensional bosonic abelian-symmetry-protected topological phases,” *Phys. Rev. B* **93**, 205157 (2016).
- [87] A. Kapustin and R. Thorngren, “Anomalies of discrete symmetries in various dimensions and group cohomology,” *ArXiv e-prints* (2014), [arXiv:1404.3230 \[hep-th\]](#).
- [88] Peng Ye and Xiao-Gang Wen, “Constructing symmetric topological phases of bosons in three dimensions via fermionic projective construction and dyon condensation,” *Phys. Rev. B* **89**, 045127 (2014).
- [89] Shang-Qiang Ning, Zheng-Xin Liu, and Peng Ye, “Symmetry enrichment in three-dimensional topological phases,” *Phys. Rev. B* **94**, 245120 (2016).
- [90] S.-Q. Ning, Z.-X. Liu, and P. Ye, “Topological gauge theory, symmetry fractionalization, and classification of symmetry-enriched topological phases in three dimensions,” *arXiv e-prints* (2018), [arXiv:1801.01638 \[cond-mat.str-el\]](#).
- [91] Peng Ye, “Three-dimensional anomalous twisted gauge theories with global symmetry: Implications for quantum spin liquids,” *Phys. Rev. B* **97**, 125127 (2018).
- [92] Juven C. Wang and Xiao-Gang Wen, “Non-abelian string and particle braiding in topological order: Modular $SL(3, \mathbb{Z})$ representation and $(3+1)$ -dimensional twisted gauge theory,” *Phys. Rev. B* **91**, 035134 (2015).
- [93] Juven C. Wang, Zheng-Cheng Gu, and Xiao-Gang Wen, “Field-theory representation of gauge-gravity symmetry-protected topological invariants, group cohomology, and beyond,” *Phys. Rev. Lett.* **114**, 031601 (2015).
- [94] Xiao Chen, Apoorv Tiwari, and Shinsei Ryu, “Bulk-boundary correspondence in $(3+1)$ -dimensional topological phases,” *Phys. Rev. B* **94**, 045113 (2016).
- [95] J. Wang, X.-G. Wen, and S.-T. Yau, “Quantum Statistics and Spacetime Surgery,” *ArXiv e-prints* (2016), [arXiv:1602.05951 \[cond-mat.str-el\]](#).
- [96] Pavel Putrov, Juven Wang, and Shing-Tung Yau, “Braiding statistics and link invariants of bosonic/fermionic topological quantum matter in $2+1$ and $3+1$ dimensions,” *Annals of Physics* **384**, 254 – 287 (2017).
- [97] Peng Ye, Meng Cheng, and Eduardo Fradkin, “Fractional s -duality, classification of fractional topological insulators, and surface topological order,” *Phys. Rev. B* **96**, 085125 (2017).
- [98] Apoorv Tiwari, Xiao Chen, and Shinsei Ryu, “Wilson operator algebras and ground states of coupled BF theories,” *Phys. Rev. B* **95**, 245124 (2017).
- [99] Kevin Walker and Zhengan Wang, “ $(3+1)$ -TQFTs and topological insulators,” *Frontiers of Physics* **7**, 150–159 (2012), [arXiv:1104.2632 \[cond-mat.str-el\]](#).
- [100] Zhi-Feng Zhang and Peng Ye, “Compatible braidings with hopf links, multi-loop, and borromean rings in $(3+1)$ -dimensional spacetime,” (2021), [arXiv:2012.13761 \[cond-mat.str-el\]](#).
- [101] Yang Qiu and Zhengan Wang, “Ground subspaces of topological phases of matter as error correcting codes,” *Annals of Physics* **422**, 168318 (2020), [arXiv:2004.11982 \[quant-ph\]](#).
- [102] D. Hardorp, *All Compact Orientable Three Dimensional Manifolds Admit Total Foliations*, American Mathematical Society: Memoirs of the American Mathematical Society (American Mathematical Society, 1980).
- [103] Frank Schindler, Ashley M. Cook, Maia G. Vergniory, Zhijun Wang, Stuart S. P. Parkin, B. Andrei Bernevig, and Titus Neupert, “Higher-order topological insulators,” *Science Advances* **4**, eaat0346 (2018), [arXiv:1708.03636 \[cond-mat.mes-hall\]](#).
- [104] Alexei Kitaev and Chris Laumann, “Topological phases and quantum computation,” (2009), [arXiv:0904.2771](#).
- [105] Meng-Yuan Li and Peng Ye, unpublished.